

# Textured window design for continuous projection stereolithography process

Yizhou Jiang<sup>a</sup>, Yilong Wang<sup>a</sup>, Ketki Lichade<sup>a</sup>, Haiyang He<sup>a</sup>, Alan Feinerman<sup>b</sup>, Yayue Pan<sup>b,\*</sup>

<sup>a</sup> Department of Mechanical and Industrial Engineering, University of Illinois at Chicago, Chicago, IL 60607, United States

<sup>b</sup> Department of Electrical and Computer Engineering, University of Illinois at Chicago, Chicago, IL 60607, United States

## ARTICLE INFO

### Article history:

Received 25 July 2019

Received in revised form 7 April 2020

Accepted 10 April 2020

Available online 11 April 2020

### Keywords:

Constrained surface design

Continuous projection stereolithography

Continuous 3D printing

Oxygen inhibition

Surface texture

## ABSTRACT

We investigate a novel textured window design for the continuous stereolithography process. The proposed textured window allows the formation of a liquid interface, enabling a reliable continuous projection stereolithography process. Both solid and hollow structures have been studied as test cases and were continuously printed using textured window-based projection stereolithography systems. The surface roughness of printed parts is characterized, and the effect of the continuous printing speed on the surface quality is investigated. Experimental results verified the effectiveness of the proposed textured window for enabling continuous printing, preventing the overlarge separation force, and achieving a high surface finish.

© 2020 Published by Elsevier Ltd on behalf of Society of Manufacturing Engineers (SME).

## 1. Introduction

Most additive manufacturing (AM) techniques build three-dimensional (3D) objects in a layer-by-layer way [1–3]. In the conventional layer-by-layer vat photopolymerization based AM processes, each layer of photosensitive resin gets polymerized by selective exposure to lights with specific wavelengths. Recently, some non-layer based vat photopolymerization techniques, including Continuous Liquid Interface Production (CLIP), High-Area Rapid Printing (HARP), CNC accumulation, and Mask Video Projection Stereolithography (MVP-SL) have been demonstrated [4–7]. Different from the conventional layer-by-layer approaches, the part is fabricated by continuously curing liquid resin through projecting a sequence of sliced images seamlessly (slice video), and meanwhile continuously pulling the part out from the resin vat, as illustrated in Fig. 1. The building speed of such continuous printing processes has been shown as an order of magnitude faster than the traditional layer-by-layer approaches, and the “staircase effect” typically found in the layer-by-layer structure were eliminated.

In these continuous printing processes, the liquid interface (a layer of liquid between the platform or cured part and the constrained window) is critical, which prevents the cured resin from

sticking to the constrained window and hence allows for continuous pulling the curing part up from the resin vat. In literature, this liquid interface has been successfully created by methods such as oxygen inhibition [4,6] and continuous liquid flow [5,7]. For example, in the CLIP process, a highly oxygen-permeable film (Teflon AF 2400, DuPont) was tensioned and clamped onto the resin vat. This Teflon film was used as an oxygen permeable constrained window, which continuously supplies oxygen to the resin during the printing process. As a result, the rich oxygen near the film inhibits the curing of the liquid resin near the film surface, forming a stable oxygen inhibition layer which works as the liquid interface for continuous printing, as illustrated in Fig. 1. The thickness of the oxygen inhibition layer can range from 20  $\mu\text{m}$  to 100  $\mu\text{m}$ , which depends on the oxygen permeability of the constrained window and the curing speed of the printing process. Some common issues, including coating failures, film tensioning failures, and creases on the film have been reported in this oxygen-permeable-film based method [8–10]. In addition to using a tensioned oxygen-permeable film as the constrained window which inhibits resin from photo-curing, the other approach to creating the liquid interface and hence enabling continuous printing is to maintain a continuous liquid flow between the curing part and the constrained window. For instance, in the HARP system [7], a continuous fluorinated oil flow on the constrained window which is the vat bottom surface works as a stable liquid interface, enabling continuous and simultaneous curing and pulling in the printing process. Such continuous oil flow also helps radiate the heat generated from the

\* Corresponding author.

E-mail addresses: [yjiang89@uic.edu](mailto:yjiang89@uic.edu) (Y. Jiang), [ywang548@uic.edu](mailto:ywang548@uic.edu) (Y. Wang), [klicha2@uic.edu](mailto:klicha2@uic.edu) (K. Lichade), [hhe20@uic.edu](mailto:hhe20@uic.edu) (H. He), [feinerman@uic.edu](mailto:feinerman@uic.edu) (A. Feinerman), [yayuepan@uic.edu](mailto:yayuepan@uic.edu) (Y. Pan).

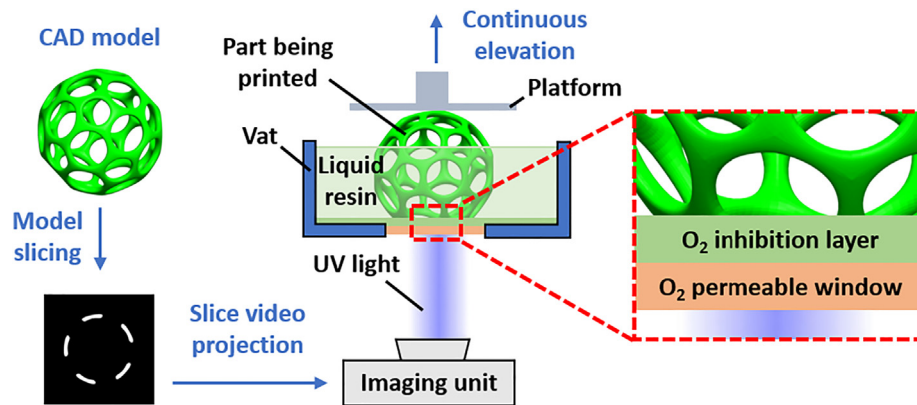


Fig. 1. Illustration of continuous printing enabled by the oxygen permeable window.

resin photo-curing, and hence allows for a rapid continuous printing speed. A potential challenge is that the oil flow needs to be delicately manipulated so that the printing quality would not be affected. An alternative method to build the continuous flow is to integrate additional robotic systems, as demonstrated by the MVP-SL process [7], in which an extra linear stage is used to achieve a continuous horizontal movement of the resin vat to enhance the resin refilling for forming and maintaining the liquid interface. A relatively large vat was utilized to accommodate the second stage motions. The control mechanism of MVP-SL is complicated, which could result in unstable resin flow and affects the curing accuracy. It should be noted that the constrained surface design of MVP-SL is based on a polydimethylsiloxane (PDMS) coated transparent glass plate. This PDMS-glass layered constrained surface provides both rigidity and elasticity, eliminating the needs of film tensioning and mechanical clamping. The relatively thick (1–2 mm) PDMS film coated on the rigid glass plate is resistant to creasing.

Although PDMS is a commonly used inexpensive and reliable material for preparing constrained windows in the photopolymerization additive manufacturing processes [11–13], the oxygen permeability of PDMS is lower than the Teflon film. Its oxygen permeability is approximately 300 barrers, while the Teflon film has a 1000 barrers oxygen permeability [4,17]. According to Dendukuri et al., the corresponding thickness of the oxygen inhibition layer provided by PDMS-glass constrained window is approximately 2.5  $\mu\text{m}$  [14], while the Teflon film window can provide up to 120  $\mu\text{m}$  thick oxygen inhibition layer without an external oxygen supply [4]. To increase the oxygen permeability of PDMS-glass constrained window, methods such as adding external oxygen supply and modifying PDMS composition have been investigated [15–18]. Yet limitations exist in these methods. Adding external devices makes the printing system bulky and changing the PDMS composition affects the PDMS elasticity and hence the printing performance.

Our previous work showed that the PDMS coated window with radial groove (RG) surface texture can enhance the liquid refilling in the conventional layer-by-layer projection stereolithography processes [19]. In addition to the RG textures, we also found that oxygen permeability can be improved by embedding air-diffusion channels (ADC) into the PDMS coated window [20]. Although these studies were focused on the layer-by-layer stereolithography process, they demonstrated the effectiveness of the RG and ADC textures on oxygen inhibition and liquid flow enhancement, implying the possible effectiveness of such textured constrained window in continuous printing. Considering the limited number of constrained windows suitable for continuous printing and their

inherent limitations, it is of great importance to investigate alternative constrained windows for continuous printing.

Against this background, this paper investigates a novel textured constrained window design, which is made of RG textured PDMS coated on an ADC-incorporated acrylic plate, for the continuous stereolithography printing. In the following sections, the effectiveness of this novel constrained window on enhancing the oxygen inhibition and continuous liquid flow in continuous printing is investigated. Both solid models and complicated hollow models are tested in this study with the proposed new constrained window. The performance of the continuous printing based on this new constrained window is discussed.

## 2. Methods and discussion

In this study, a continuous projection SL setup was developed, as illustrated in Fig. 2a. The imaging unit used in this study was Wintech PRO4500 with a 25.4 mm diameter lens (WDST-3P-PRO4500, Texas Instruments). Fig. 2b shows the schematic drawing of the resin vat with ADC-RG textures. The ADC-RG textured window consists of an acrylic plate incorporated with air-diffusion channels and a 2.0 mm layer of radial-groove textured PDMS coating on top of the acrylic plate. Both the air diffusion channels on the acrylic plate and the radial groove pattern on the PDMS surface were fabricated by laser micromachining (X2-600 100-watt CO<sub>2</sub> laser system, Universal Laser Systems, USA). For RG textures used in this study, we adopted 250  $\mu\text{m}$  radial groove width, 150  $\mu\text{m}$  radial groove depth, and 30° angular spacing between adjacent grooves, as shown in Fig. 2c. Such RG design parameter setting was found to be capable of enhancing the resin flow in our previous work [19].

To investigate the effect of the air-diffusion channels on the oxygen permeability, the oxygen inhibition layers with varied channel diameters were measured using a UV light with  $135 \pm 5$  mV intensity (405 nm wavelength) [21]. The liquid photopolymer used in this study was MakerJuice Labs G + . The air-diffusion channels were arranged into arrays on the constrained surface with a 2.0 mm channel-to-channel distance. A differential approach was utilized to calibrate the oxygen inhibition layer thickness [20], in which the liquid photopolymer was first sandwiched between the constrained window and an impermeable glass with two 500  $\mu\text{m}$  thick brass shims supporting them. Then, the imaging unit projected a 5 mm diameter solid circle to the constrained window for 30 sec. Accordingly, a cylinder model of 5 mm diameter was cured. The oxygen inhibition layer thickness was then computed by differentiating the cured cylinder thickness

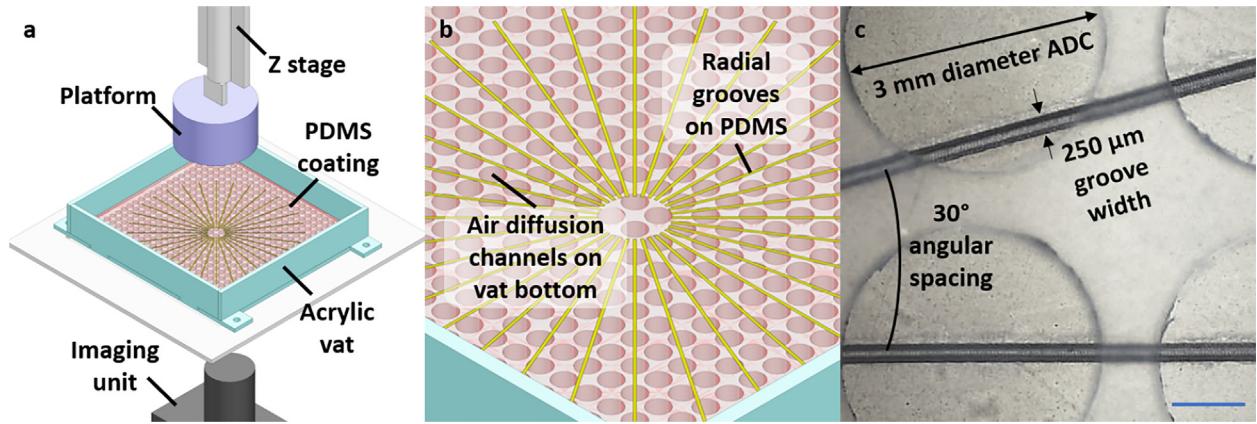


**Fig. 2.** Textured window design. a) Schematic drawing of the SL setup. b) Schematic drawing of the resin vat with integrated ADC-RG constrained surface design. c) Bottom view optical image of the proposed ADC-RG design, scale bar = 1 mm.

from the shim thickness (500 μm). ADC-RG constrained windows with a channel diameter ranging from 0.20 to 0.80 mm were tested. As shown in Fig. 3a, the oxygen inhibition layer thickness was found to be proportional to the ADC diameter. Specifically, the constrained window with 0.8 mm diameter air-diffusion channels can produce an approximately 100 μm thick oxygen inhibition layer, which is comparable to the one created by the highly oxygen permeable Teflon film AF 2400 used in the CLIP process [4], implying the feasibility of the proposed ADC-RG constrained window design for the continuous printing process.

During the continuous printing process, it is critical to maintain the liquid interface, which requires a proper continuous printing speed (pulling speed) matching with the photopolymer curing speed. Otherwise, printing defects such as weak-bonding (printing too fast) and over-curing (printing too slow) may occur. In this study, the time-dependent curing depth of the liquid resin was characterized, as shown in Fig. 3b. Results indicated that the curing depth ranged from 0.20 to 0.32 mm when the projecting time increased from 4 to 9 sec, which gave an approximately 75 mm/h estimated curing speed. To further understand the relationship

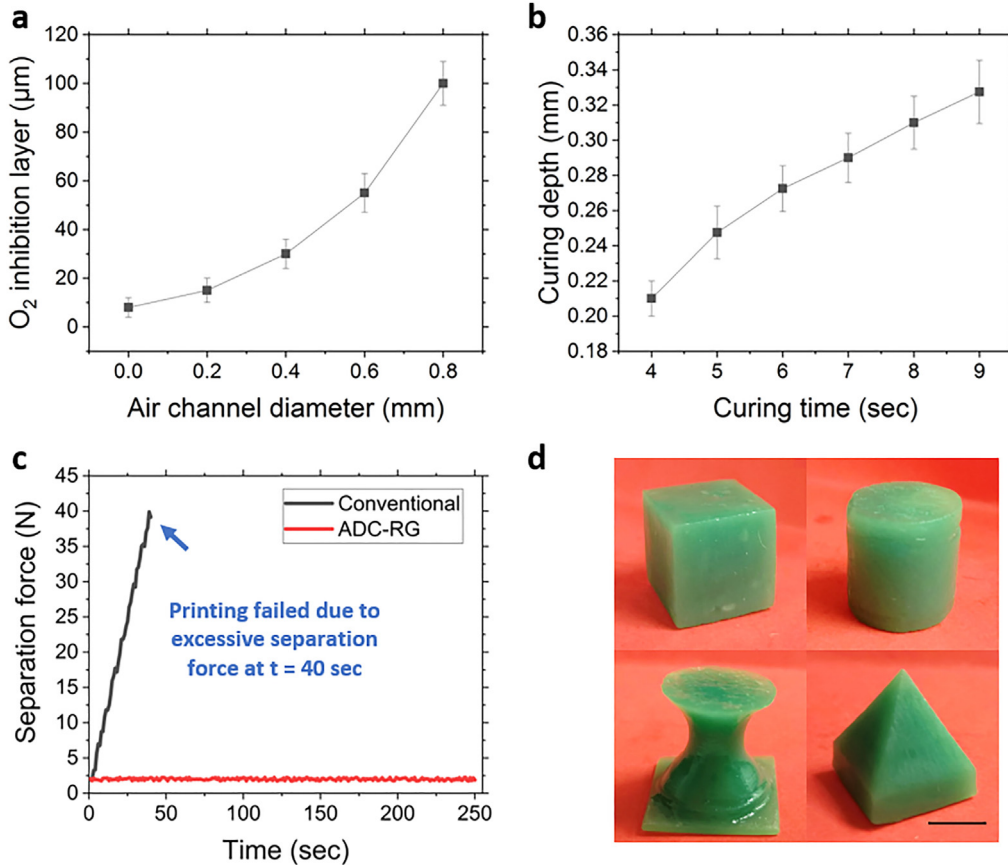


**Fig. 3.** Oxygen inhibition layer and separation force. a) Measured oxygen inhibition layer thickness under various ADC diameters. b) Measured curing depth of MakerJuice G + resin using a 405 nm wavelength UV light. c) Separation force comparison between plain PDMS surface and ADC-RG textured surface when printing 10 mm height and 10 mm diameter cylinder. d) Printed solid parts, scale bar = 5 mm.

between the printing speed and the printing quality, we investigated the ADC-RG constrained window based continuous printing process with a printing speed ranging from 50% to 150% of the estimated resin curing speed in the following test cases.

Cylinder models with 10 mm height and 10 mm diameter ( $78.5 \text{ mm}^2$  cross-sectional area) were continuously printed at a 144 mm/hour printing speed, and the pulling force was recorded using a force-detection system [19]. The system consisted of a load cell (LRM 200, Futek) and a data acquisition (DAQ) device (USB 6008, National Instruments). The real-time pulling force was monitored in the integrated Matlab/Simulink unit. Here, we tested both non-textured PDMS-acrylic constrained window and ADC-RG (0.8 mm ADC diameter,  $250 \mu\text{m}$  radial groove width,  $150 \mu\text{m}$  radial groove depth, and  $30^\circ$  angular spacing between adjacent grooves) textured PDMS-acrylic constrained window. As shown in Fig. 3c, the printing stopped due to an excessive pulling force (40.2 N) at 40 s when using the non-textured constrained window. This excessive force occurred because the liquid interface had been depleted and as a result the over-cured resin adhered to the constrained window. Using the ADC-RG textured constrained window, the 10 mm wide solid cylinder was fabricated in 250 s without defects, as shown in Fig. 3d. The pulling force during the whole continuous printing process was only up to 2.7 N, indicating that the ADC-RG texture created and maintained a sufficient liquid interface for preventing the adhesion problem in continuous printing of solid objects, and several solid models including cube, spline, and pyramid were printed under the same setting (Fig. 3d).

In addition to the solid models, a 22.5 mm diameter cage model was also continuously printed using this novel ADC-RG textured constrained window. Speeds of 45.0 mm/h, 67.5 mm/h, 90.0 mm/h, and 112.5 mm/h were tested. The parts printed with these speeds were observed under a microscope, as shown in Fig. 4a.

The surface finish of these printed parts was characterized by a surface roughness tester (GT-K Optical Profiler, Bruker). The grayscale mappings of the surface roughness and the variations in surface height are shown in Fig. 4b and 4c. Results indicated that models printed at 45.0 mm/h and 67.5 mm/h show similar surface finish with a measured ten-point mean roughness ( $R_z$ ) of  $11.1 \mu\text{m}$  and  $26.5 \mu\text{m}$ , respectively. However, with the printing speed increased to 90.0 mm/h, undesired pores were formed on the printed structure. The diameter of pores ranges from 100 to  $500 \mu\text{m}$ , leading to a rougher and porous surface with a measured  $R_z$  of  $40.6 \mu\text{m}$ . The printing quality became worse when the printing speed increased to 112.5 mm/h. The undesired void contents are mainly caused by the incomplete photopolymerization within the rapid resin flow at a relatively fast printing speed. It indicates that the continuous printing speed, which is the speed to pull the part out of the resin, should be no larger than the curing speed. The experimental results validated that the ADC-RG constrained window is effective for continuous printing of solid structures and complicated hollow structures, with a maximum printing speed close to the photopolymer curing speed.

### 3. Conclusion

This paper investigated a novel ADC-RG textured constrained window design for the continuous projection stereolithography process. The design consists of patterned air-diffusion channels (ADC) incorporated in an acrylic plate and radial groove (RG) patterns textured on a PDMS layer which is coated on the acrylic plate. The ADC-RG textured constrained window exhibited the capability of forming and maintaining an effective liquid interface ( $\sim 100 \mu\text{m}$  oxygen inhibition layer) to enable the continuous printing process.

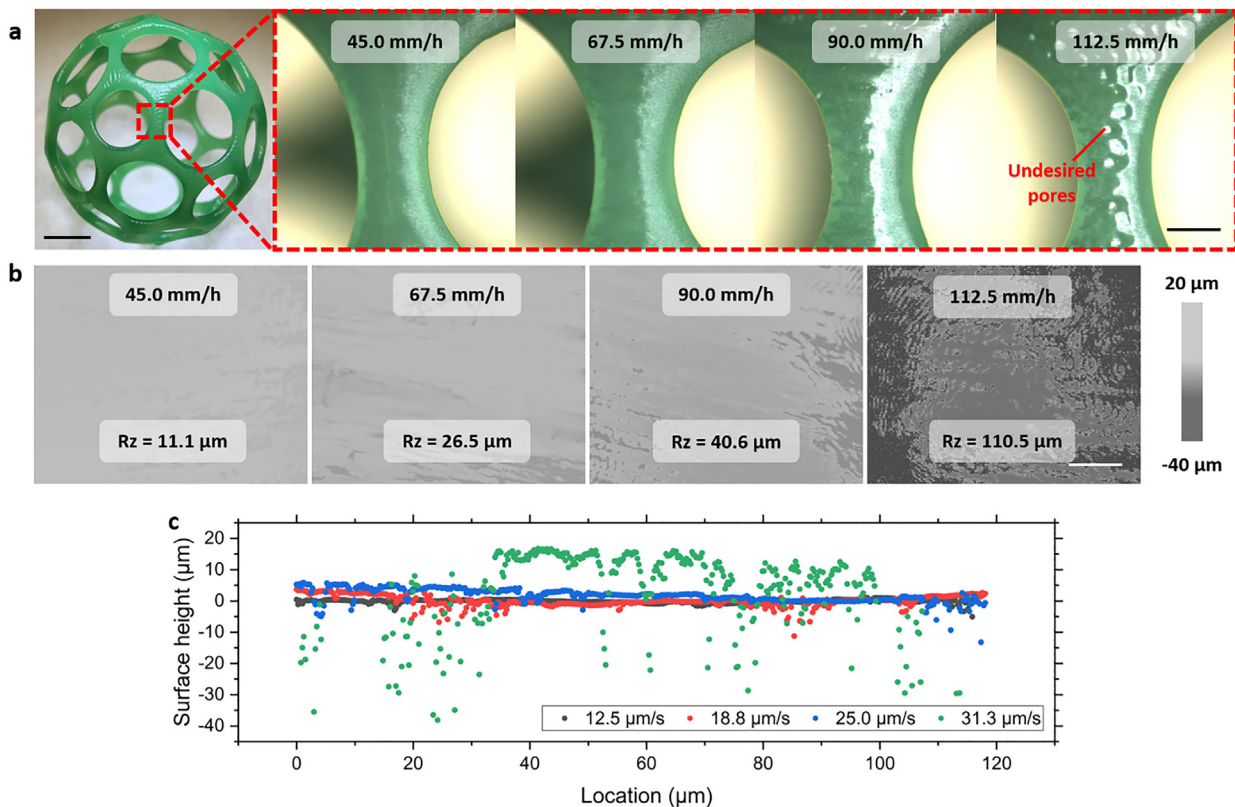


Fig. 4. Printed part surface quality under varied printing speeds. a) Optical and microscope images: left scale bar = 5 mm, right scale bar = 1 mm. b) Surface roughness grayscale mappings, scale bar =  $30 \mu\text{m}$ . c) Surface roughness raw data.

Compared with the conventional non-textured constraint window, the ADC-RG texture can significantly ease the pulling to avoid adhesion failures. A small surface roughness  $R_z$  ( $\sim 11 \mu\text{m}$ ) was observed in the printed parts. Experimental results validated the feasibility and effectiveness of the ADC-RG constrained window on continuous printing of both solid structures and complicated hollow structures at moderate sizes and ultra-high speeds. Future work will focus on investigating the integration of this textured window with other existing methods with the aim of achieving continuous printing of wide solid structures.

### Declaration of Competing Interest

The authors declare that they have no known competing financial interests or personal relationships that could have appeared to influence the work reported in this paper.

### Acknowledgement

The authors acknowledge the support from National Science Foundation (NSF) under Grant 1563477. The authors would like to also acknowledge the Nanotechnology Core Facility (NCF) of the University of Illinois at Chicago campus for the use of the Bruker GT-K Optical Profilometer.

### References

- [1] Edgar J, Tint S. Additive manufacturing technologies: 3D printing, rapid prototyping, and direct digital manufacturing. *Johnson Matthey Technol Rev* 2015;59(3):193–8.
- [2] Gibson I, Rosen DW, Stucker B. Additive manufacturing technologies, Vol. 17. New York: Springer; 2014.
- [3] Bártolo PJ, editor. Stereolithography: materials, processes and applications. Springer Science & Business Media; 2011.
- [4] Tumbleston JR, Shirvanyants D, Ermoshkin N, Januszewicz R, Johnson AR, Kelly D, et al. Continuous liquid interface production of 3D objects. *Science* 2015;aaa2397.
- [5] Li X, Mao H, Pan Y, Chen Y. Mask video projection-based stereolithography with continuous resin flow. *J Manuf Sci Eng* 2019;141(8):081007.
- [6] Bourell D, Stucker B, Chen Y, Zhou C, Lao J. A Layerless additive manufacturing process based on CNC accumulation. *Rapid Prototyping J* 2011.
- [7] Walker DA, Hedrick JL, Mirkin CA. Rapid, large-volume, thermally controlled 3D printing using a mobile liquid interface. *Science* 2019;366(6463):360–4.
- [8] Liravi F, Das S, Zhou C. Separation force analysis and prediction based on cohesive element model for constrained-surface Stereolithography processes. *Comput Aided Des* 2015;69:134–42.
- [9] Gritsenko D, Yazdi AA, Lin Y, Hovorka V, Pan Y, Xu J. On characterization of separation force for resin replenishment enhancement in 3D printing. *Addit Manuf* 2017;17:151–6.
- [10] Pan Y, He H, Xu J, Feinerman A. Study of separation force in constrained surface projection stereolithography. *Rapid Prototyping J* 2017;23(2).
- [11] Zhou C, Chen Y, Yang Z, Khoshnevis B. Digital material fabrication using mask-image-projection-based stereolithography. *Rapid Prototyping J* 2013;19(3):153–65.
- [12] Ye H, Venkateswaran A, Das S, Zhou C. Investigation of separation force for constrained-surface stereolithography process from mechanics perspective. *Rapid Prototyping J* 2017;23(4):696–710.
- [13] Pan Y, Chen Y, 2013. Fast Micro-Stereolithography Process based on Bottom-up Projection for Complex Geometry. In: Proceedings of the 8th International Conference on Micro Manufacturing, ICOMM 2013, pp. 1–8.
- [14] Dendukuri D, Pregibon DC, Collins J, Hatton TA, Doyle PS. Continuous-flow lithography for high-throughput microparticle synthesis. *Nat Mater* 2006;5(5):365–9.
- [15] Thomas PC, Raghavan SR, Forry SP. Regulating oxygen levels in a microfluidic device. *Anal Chem* 2011;83(22):8821–4.
- [16] Leclerc E, Sakai Y, Fujii T. Microfluidic PDMS (polydimethylsiloxane) bioreactor for large-scale culture of hepatocytes. *Biotechnol Prog* 2004;20(3):750–5.
- [17] Lamberti A, Marasso SL, Cocuzza M. PDMS membranes with tunable gas permeability for microfluidic applications. *RSC Adv* 2014;4(106):61415–9.
- [18] Shiku H, Saito T, Wu CC, Yasukawa T, Yokoo M, Abe H, et al. Oxygen permeability of surface-modified poly (dimethylsiloxane) characterized by scanning electrochemical microscopy. *Chem Lett* 2006;35(2):234–5.
- [19] He H, Xu J, Yu X, Pan Y. Effect of Constrained Surface Texturing on Separation Force in Projection Stereolithography. *J Manuf Sci Eng* 2018;140(9):091007.
- [20] He H, Pan Y, Feinerman A, Xu J. Air-diffusion-channel constrained surface based stereolithography for three-dimensional printing of objects with wide solid cross sections. *ASME. J. Manuf. Sci. Eng.* 2018;140(6).
- [21] Januszewicz R, Tumbleston JR, Quintanilla AL, Mecham SJ, DeSimone JM. Layerless fabrication with continuous liquid interface production. *Proc Natl Acad Sci* 2016;113(42):11703–8.